



Summer Project Report

Bianka Wołoncewicz

University of Gdańsk, Poland

Abstract

Modeling of all photoinduced processes during x-ray irradiation of high atomic number samples is computationally very challenging, due to a large number of electronic configurations and transitions to be followed. We propose an approximate approach where only most probable configurations and transitions are followed such that the ionization dynamics mimic the average behavior of the full system. A comparison to the full system simulation is presented.

Contents

1	Introduction	3
2	Algorithm	4
3	Analysis of chosen elements	4
4	Error estimates and optimal branching	7
5	Conclusions	13

1 Introduction

Plasma is one of the four fundamental states of the matter. It contains significant amount of charge carriers and interacts strongly with electromagnetic field. We believe that around 99% of the universe is made up of plasma. It can be found in all type of stars and within giants planets. Nowadays we are able to create it in laboratories by exposing samples to high power light sources such as, e.g., XFELs (X-ray Free Electron Lasers) - apart from other conventional discharge methods. We can study plasma properties, compare theoretical models with experimental data and follow plasma evolution in time. One of the aspects of these investigations is the interaction of atoms with hard x-ray radiation. The focus of the current study is on Auger processes and photoionization during the plasma creation.

Modeling of all photoinduced processes during x-ray irradiation of high atomic number samples is computationally very challenging, due to a large number of electronic configurations and transitions to be followed. We propose an approximate approach where only most probable configurations and transitions are followed such that the ionization dynamics mimic the average behavior of the full system. For our studies we utilize the XATOM code. XATOM [1, 2] is a tool that uses the Hartree-Fock-Slater model [3] and calculates rates and cross sections of any x-ray-induced processes for any element within a non-relativistic framework.

To illustrate the complexity of the planned calculations, we first used XATOM program to find all possible configurations for C ($Z = 6$) interacting with hard X-ray photons. This information can be used in Boltzmann simulation [4, 5] to increase its computational efficiency. For heavy elements ($Z > 13$) the computation including all transitions and configurations is very time-consuming. For higher Z it becomes practically impossible. That is why we are working on the reduction of the number of processes and configurations involved in the calculations. We attempt to approximate a full computation with a chain of transitions that consists of the most probable photoionization and Auger processes, involving much smaller number of configurations. Such a chain should be relatively short and give total charge evolution in time close to the average one obtained from full calculation, $\langle Q(t)_{full} \rangle$. The charge, $Q(t)$, denotes here the total number of free electrons present in the sample at a time, t . Below we consider various methods of choosing the most optimal chain. The algorithm for picking out transitions is based on Monte Carlo simulation, so that the chain consists of the transitions chosen randomly, according to the rates for Auger processes and cross section for photoionization.

2 Algorithm

Our calculations should be applicable for pulses with time-dependent intensity. For our modeling we assume the gaussian pulse. In experiments SASE pulse is used but over many shots the SASE pulse shape averages to a gaussian one. Our intensity range corresponds to the one used in plasma experiments which is between 10^{13} - 10^{19} [W/cm²]. Our time range corresponds to the chosen pulse.

We scan the intensity range between the minimal and maximal intensities to identify the optimal chain of transitions, i.e., yielding the charge closest to the $\langle Q(t)_{full} \rangle$. Each (constant) intensity is used to calculate one branch of transitions. Various branches, each corresponding to one scanned intensity, are then merged in a chain. The chain is then optimized in the following steps:

1. Branches for different intensities are randomly calculated. Combined chain is then formed out of them.
2. The $Q(t)$ evolution is calculated for each chain.
3. The average $\langle Q(t) \rangle$ is calculated.
4. The chain is selected for which $Q(t) \equiv Q(t)_{sel}$ is closest to the average $\langle Q(t) \rangle$.

Once the optimal chain is chosen we compare it with $\langle Q(t)_{full} \rangle$ obtained from a full simulation including all processes and calculate the maximal relative error (ΔQ):

$$\Delta Q = \max_t \frac{|Q(t)_{sel} - \langle Q(t)_{full} \rangle|}{\langle Q(t)_{full} \rangle}. \quad (1)$$

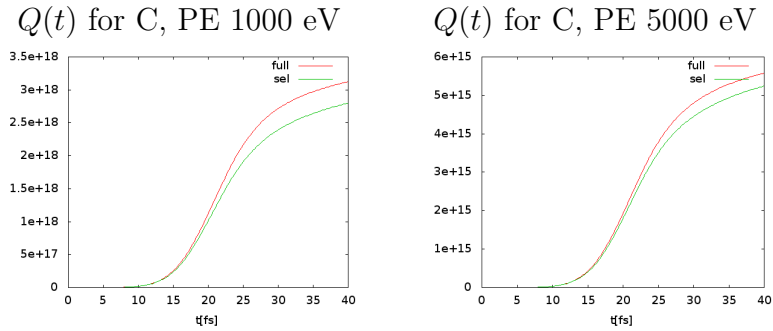
3 Analysis of chosen elements

We analyzed biologically relevant elements such as: C ($Z = 6$), N ($Z = 7$), O ($Z = 8$), Mg ($Z = 12$), S ($Z = 16$) and elements important for plasma research Al ($Z = 13$), Ti ($Z = 22$) for the photon energies (PE) of 1000 eV and 5000 eV. All calculations have been performed on other elements as well (not shown; details in the Appendix left with the supervisors). In the Table 1 we show the maximal relative error obtained for the fixed number of configurations used in the selected chain.

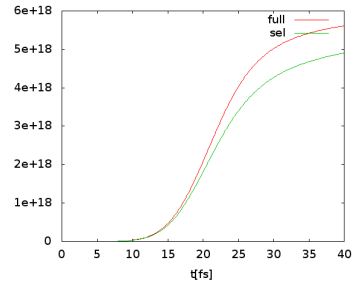
Table 1: Elements, photon energy, number of all and selected configurations and maximal relative error

Element	PE (eV)	All config.	Selected config.	Maximal rel. error
C	1000	27	10	0.119420
	5000		11	0.114090
N	1000	36	14	0.156768
	5000		18	0.083292
O	1000	45	13	0.159942
	5000		18	0.077715
Mg	1000	189	21	0.091793
	5000		30	0.115228
Al	1000	478	20	0.183658
	5000		21	0.145215
S	1000	945	45	0.338320
	5000		39	0.177697
Ti	1000	6615	75	0.518374
	5000		69	0.344859

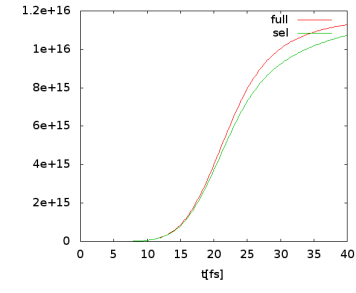
The following plots present $Q(t)$ evolution of C for the photon energies (PE) 1000 eV and 5000 eV. Our time range is 40 fs, which corresponds to the pulse duration.



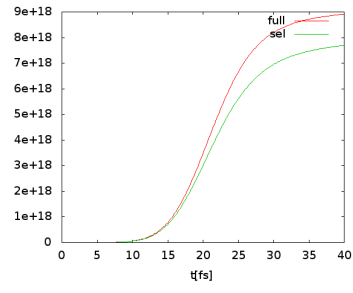
$Q(t)$ for N, PE 1000 eV



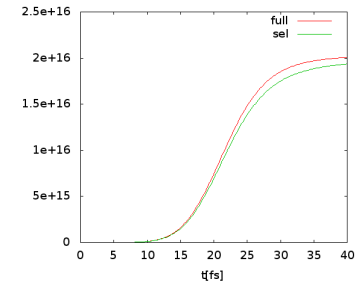
$Q(t)$ for N, PE 5000 eV



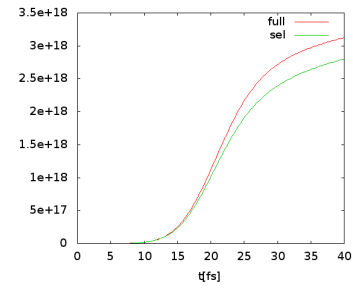
$Q(t)$ for O, PE 1000 eV



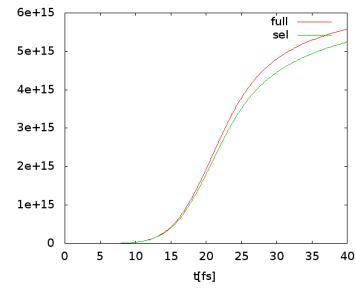
$Q(t)$ for O, PE 5000 eV



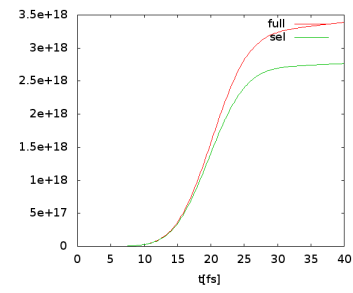
$Q(t)$ for Mg, PE 1000 eV



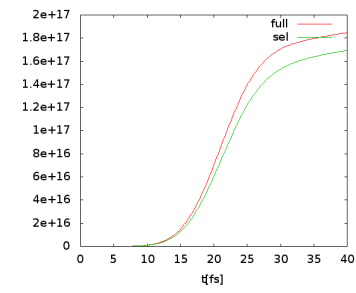
$Q(t)$ for Mg, PE 5000 eV

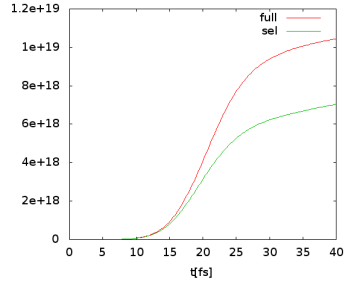
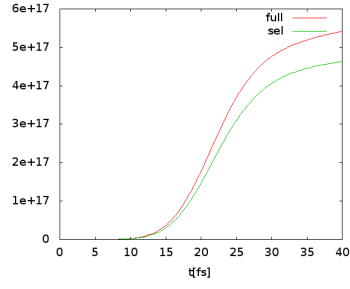
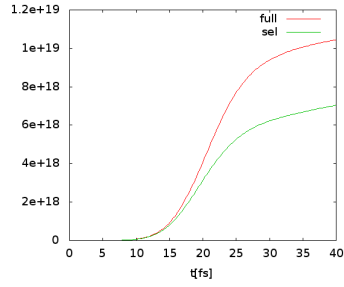
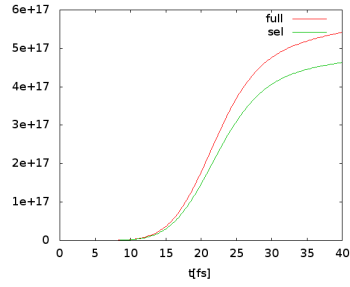


$Q(t)$ for Al, PE 1000 eV



$Q(t)$ for Al, PE 5000 eV



$Q(t)$ for S, PE 1000 eV $Q(t)$ for S, PE 5000 eV $Q(t)$ for Ti, PE 1000 eV $Q(t)$ for Ti, PE 5000 eV

The goal of reducing the number of configurations has been achieved but the maximal relative error is quite significant. The aim of further analysis is to reduce this error.

4 Error estimates and optimal branching

After many computational experiments we found that we can reduce the error by increasing the number of intensity branches. The more branches we include, the more transitions are considered, and the $Q(t)_{sel}$ approaches better the $\langle Q(t)_{full} \rangle$. On the other hand by increasing the number of intensity branches we increase the number of transitions and configurations, which is discrepant with our need of minimizing the chain. Therefore we need to find a compromise between reducing the error and increasing the number of intensity brunches, picking up the optimal result. The following plot presents the dependence of maximal relative error on the number of included intensity branches for C at photon energy of 1000 eV.

Carbon at PE 1000 eV

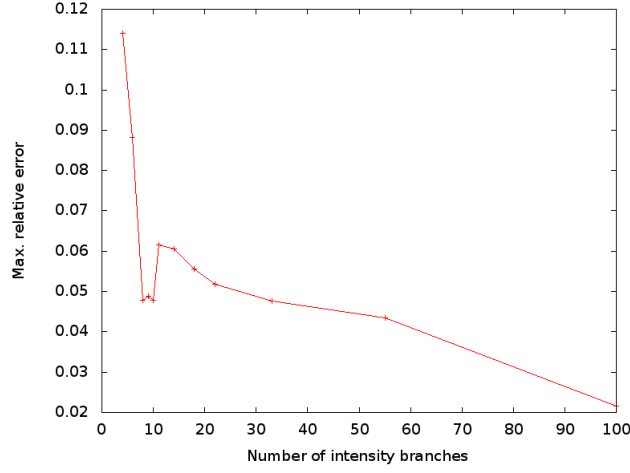


Figure 1: Error and number of intensity branches for C at PE 1000 eV

We observe that the dependence between the error and number of intensity branches is nonlinear. We test carefully the dependence in the range of number of intensity branches that may seem convenient for calculations. The results are presented in the table below.

Table 2: Intensity branches, processes and configurations for C PE 1000 eV

no of int. branches.	sel. processes	all proc.	sel. config.	all config.	max.rel.error
4	9	74	9	27	0.120183
6	16	74	13	27	0.088209
10	20	74	15	27	0.077660
14	22	74	17	27	0.060466
18	14	74	11	27	0.055522

We could pick up a chain of 18 intensity branches that includes 11 out of 27 configurations and the maximal relative error is about 5%. That result is quite satisfying as for the moment in our approach the smallest number of configurations achieved for an optimal chain was 10.

Carbon at PE 5000 eV

We repeated the same analysis for carbon irradiated with photons of energy 5000 eV. We could see that the error decreased, while the photon energy increased.

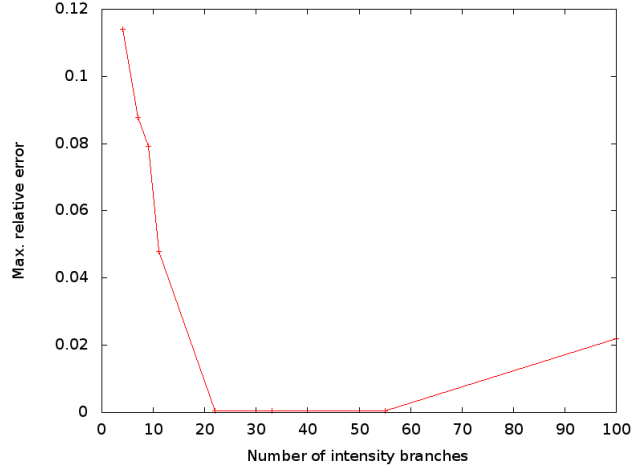


Figure 2: Error and number of intensity branches for C at PE of 5000 eV

Table 3: Intensity branches, processes and configurations for C at PE of 5000 eV

no of int. branches.	sel. processes	all proc.	sel. config.	all config.	max.rel.error
4	10	74	10	27	0.114090
8	14	74	12	27	0.047844
10	16	74	13	27	0.047844
14	16	74	13	27	0.047844
18	14	74	11	27	0.000454

Again we can pick up the optimized chain that includes 18 intensity branches and it gives a very precise approximation of $Q(t)$ evolution with the maximal relative error of ~ 0.0004 .

In the following part of this report the results Al and Ti are presented. Let us observe how the error can be reduced and how it influences the number of configurations that are used in the optimal chain. Please refer to the Appendix in order to see similar analysis of other elements.

Aluminum at PE of 1000 eV

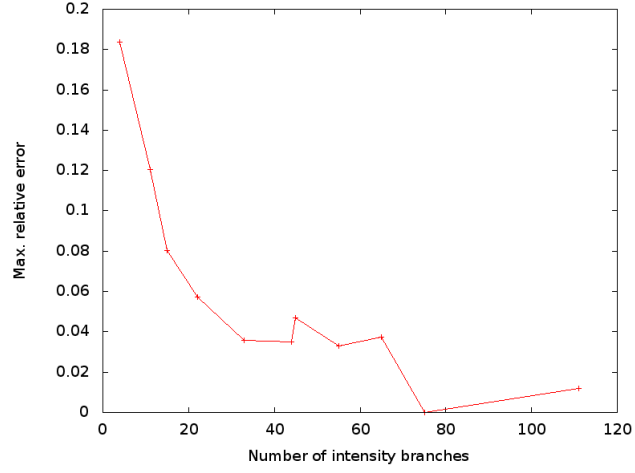


Figure 3: Error and number of intensity branches for Al, PE 1000eV

Table 4: Intensity branches, processes and configurations for Al, PE 1000 eV

no of int. branches.	sel. processes	all proc.	sel. config.	all config.	max.rel.error
4	24	2688	20	478	0.183658
15	63	2688	59	478	0.080313
45	93	2688	57	478	0.047087
65	109	2688	62	478	0.037343

The optimal chain that contains 65 intensity branches, includes 62 configurations (that is about 13% of all configurations). The error achieved is about 3%.

Aluminum at PE of 5000 eV

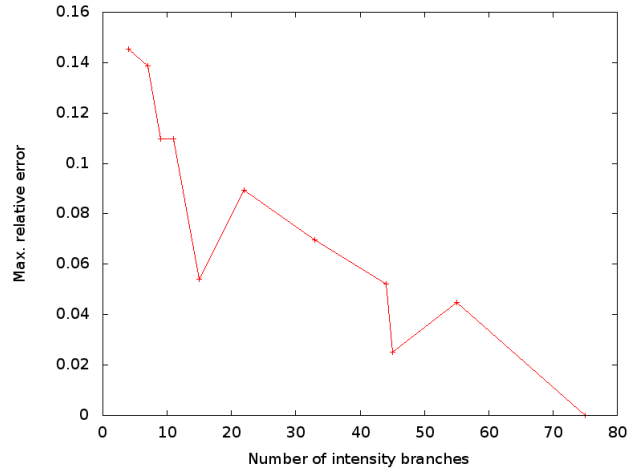


Figure 4: Error and number of intensity branches for Al at PE of 5000 eV

Table 5: Intensity branches, processes and configurations for Al at PE of 5000 eV

no of int. branches.	sel. processes	all proc.	sel. config.	all config.	max.rel.error
4	26	2688	21	478	0.145215
15	70	2688	56	478	0.054098
45	125	2688	86	478	0.025223
75	151	2688	101	478	0.018403

Titanium at PE of 1000 eV

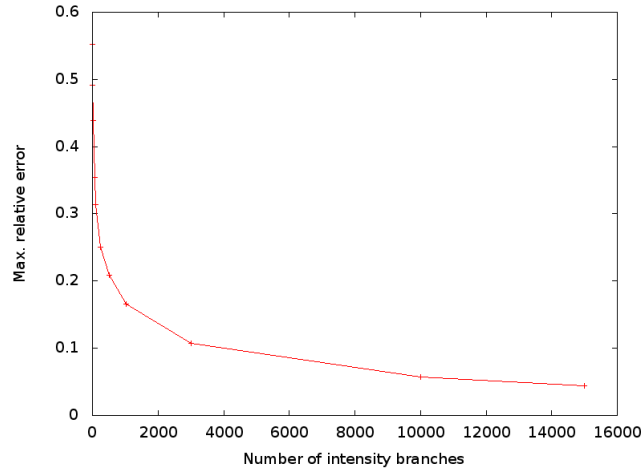


Figure 5: Error and number of intensity branches for Ti, PE 1000 eV

Table 6: Intensity branches, processes and configurations for Ti PE 1000 eV

no of int. branches.	sel. processes	all proc.	sel. config.	all config.	max.rel.error
100	460	48884	304	6615	0.313164
3000	2520	48884	996	6615	0.107120
10000	4231	48884	1343	6615	0.056913
15000	4901	48884	1444	6615	0.044488

Titanium at PE of 5000 eV

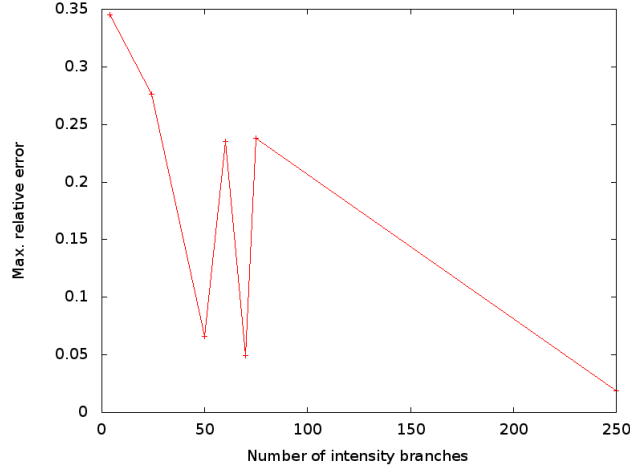


Figure 6: Error and number of intensity branches for Ti, PE 5000 eV

Table 7: Intensity branches, processes and configurations for Ti PE 5000 eV

no of int.branches.	sel. processes	all proc.	sel. config.	all config.	max.rel.error
4	79	145105	69	6615	0.344859
50	370	145105	244	6615	0.066161
250	807	145105	399	6615	0.019124

5 Conclusions

Our approach may be used in order to minimize the number of configurations and transitions following the photoionization of an atom interacting with hard X-rays. We were always able to reduce the maximal relative error up to 1% by increasing the number of intensity branches. Unfortunately, there is a trade-off between the number of configurations and the maximal relative error which for heavier elements ($Z > 13$) increases significantly. On the other hand by analyzing carefully the dependence between the error and number of intensity branches we were always able to find a compromise solution that may be used in further calculations. The following plot presents the dependence of the atomic number Z on the number of selected configurations in the optimized chain at the fixed maximal relative error of 5 – 6%. We observe the exponential growth.

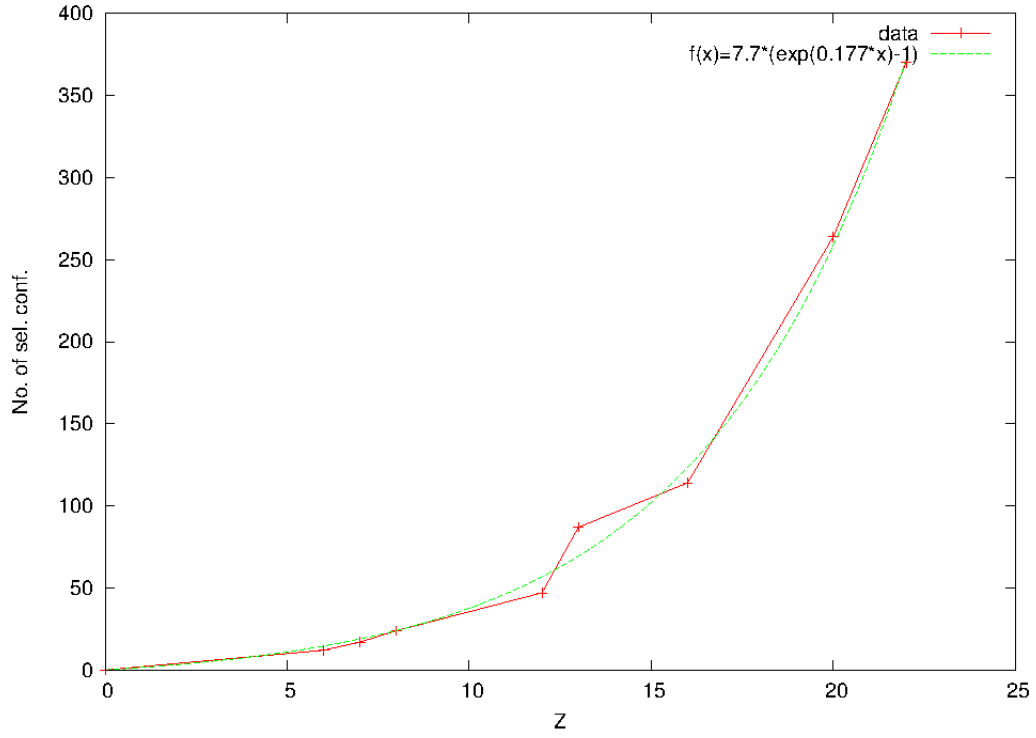


Figure 7: Atomic number Z and the number of selected configurations in the optimized chain

References

- [1] Sang-Kil Son and Robin Santra, XATOM, an integral toolkit for x-ray and atomic physics, CFEL, DESY, Hamburg, Germany 2013, revision 972.
- [2] Sang-Kil Son, R. Thiele, Z. Jurek, B. Ziaja, R. Santra, Phys. Rev. X, 4, 031004 (2014).
- [3] J. C. Slater, Phys. Rev. 81(3), 385 (1951).
- [4] B. Ziaja et al., Eur. Phys. J. D 40, 456-480 (2006).
- [5] B. Ziaja et al., In preparation.
- [6] I. Sobelman, Introduction to the atomic spectra.